INTERNATIONAL JOURNAL FOR NUMERICAL METHODS IN FLUIDS, VOL. 7, 17–27 (1987)

FINITE ELEMENT STREAM FUNCTION–VORTICITY SOLUTIONS OF THE INCOMPRESSIBLE NAVIER–STOKES EQUATIONS

M. F. PEETERS*

Pratt & Whitney Canada, Mississauga, Ontario, Canada

W. G. HABASHI†

Concordia University, Montreal, Quebec, Canada

AND

E. G. DUECK‡

Pratt & Whitney Canada, Mississauga, Ontario, Canada

SUMMARY

The incompressible, two-dimensional Navier–Stokes equations are solved by the finite element method (FEM) using a novel stream function/vorticity formulation. The no-slip solid walls boundary condition is applied by taking advantage of the simple implementation of natural boundary conditions in the FEM, eliminating the need for an iterative evaluation of wall vorticity formulae. In addition, with the proper choice of elements, a stable scheme is constructed allowing convergence to be achieved for all Reynolds numbers, from creeping to inviscid flow, without the traditional need for upwinding and its associated false diffusion. Solutions are presented for a variety of geometries.

KEY WORDS Finite Element Navier–Stokes Stream Function Vorticity

INTRODUCTION

Considerable effort has been devoted to methods for solving the two-dimensional Navier–Stokes equations. The problem is generally studied using formulations based on primitive variables (u, v, p), stream function/vorticity (Ψ, ω) or stream function alone. In this study a stream function/vorticity formulation is used.

Traditional (Ψ, ω) formulations impose the Dirichlet boundary condition of Ψ (no-penetration) on the stream function equation while iteratively applying approximate wall vorticity formulae to try to satisfy the no-slip condition. This approach is generally limited to low Reynolds number (Re) flows unless some form of upwinding and its associated false diffusion is introduced.

Campion-Renson and Crochet[1] have outlined a finite element method that solves the equations simultaneously, without the use of wall vorticity formulae. Their results were, however, only presented for Re up to 400 for the driven cavity problem and 50 for a forward facing step.

Dhatt *et al.*[2] developed a formulation in which the Dirichlet boundary condition is imposed

* Senior Aerodynamicist
† Professor; Consultant, Pratt & Whitney Canada
‡ Chief, Turbofan Aerodynamics

0271–2091/87/010017–11$05.50

Received July 1985
Revised 5 May 1986

on the stream function equation while the vorticity transport equation is replaced by an explicit finite element approximation of the no-slip condition. Results were obtained for very high Re without the need for upwinding. It will be shown that their choice of element was the key to obtaining high Re solutions.

In this paper we examine the linear problem of Stokes flow ($Re = 0$), for which a variational principle exists, and show that the Dirichlet boundary condition on Ψ replaces the vorticity transport equation at solid walls while the no-slip condition is satisfied naturally by the stream function equation. The method, although paralleling the development of Campion-Renson and Crochet, is capable, with proper choices of elements and grids, of extending the solutions to all Reynolds numbers without the need for upwinding.

The finite element method advantages are made even more evident in the solution of the pressure field. A Poisson type pressure equation is obtained by taking the divergence of the momentum equations. This formulation[3] is somewhat different from those commonly found in the literature and leads to very simple boundary conditions, particularly suited to finite elements.

Solutions are presented for the classical driven cavity problem as well as for more complex geometries, demonstrating the ease with which the method handles complex geometries.

GOVERNING EQUATIONS

For two-dimensional steady, incompressible, laminar flows, the vorticity is defined as

$$\omega = \nabla \times \mathbf{u}, \tag{1}$$

$\mathbf{u}$ being the velocity vector. The vorticity transport equation is obtained by taking the curl of the momentum equation. Defining a stream function Ψ such that

$$u = \partial\Psi/\partial y; \quad v = -\partial\Psi/\partial x,$$

ensures that continuity is automatically satisfied. The definition of vorticity in terms of stream function thus becomes

$$\nabla^2\Psi + \omega = 0, \tag{2}$$

and the vorticity transport equation is

$$\nabla^2\omega - Re(\Psi_y\omega_x - \Psi_x\omega_y) = 0. \tag{3}$$

Equations (2) and (3) are the equations to be solved.

The problem is solved in the domain D bounded by the curve C. C can be broken up into 3 types C_1, C_2, C_3. C_1 corresponds to solid walls where the velocity must be specified; thus Ψ and Ψ_n are given. C_2 corresponds to the inlet where both Ψ and ω are specified and C_3 corresponds to the exit where the streamwise derivatives of both Ψ and ω are assumed to be zero. The boundary conditions are summarized as follows:

$$(x, y)\in C_1, \quad \Psi(x, y) = \bar{\Psi}(s), \quad \Psi_n(x, y) = \bar{\Psi}_n(s), \tag{4a}$$

$$(x, y)\in C_2, \quad \Psi(x, y) = \bar{\Psi}(s), \quad \omega(x, y) = \bar{\omega}(s), \tag{4b}$$

$$(x, y)\in C_3, \quad \Psi_n(x, y) = 0, \qquad \omega_n(x, y) = 0. \tag{4c}$$

Figure 1 illustrates a typical problem exhibiting all three types of boundaries.

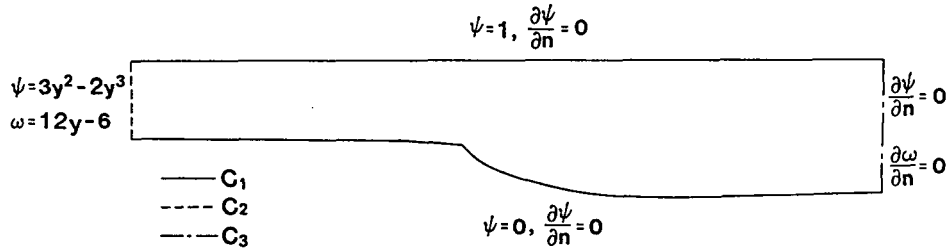

Figure 1. Boundary conditions on C_1, C_2 and C_3

FINITE ELEMENT FORMULATION

Variational method for Stokes flow ($Re = 0$).

One of the major difficulties with (Ψ, ω) formulations is the boundary condition on solid walls (C_1). On this boundary there are two conditions on Ψ and none on ω. To gain insight into how to deal with this problem it is instructive to outline the formulation for Stokes flow, for which a variational principle exists:

$$I = \iint [-(\nabla\omega)\cdot(\nabla\Psi) + \tfrac{1}{2}\omega^2]\,d\sigma + \int \omega\Psi_n\,ds + \int \Psi\omega_n\,ds. \tag{5}$$

Using Green's theorem, equation (5) can be rewritten as

$$I = \iint [\omega\nabla^2\Psi + \tfrac{1}{2}\omega^2]\,d\sigma + \int \Psi\omega_n\,ds, \tag{6a}$$

$$I = \iint [\Psi\nabla^2\omega + \tfrac{1}{2}\omega^2]\,d\sigma + \int \omega\Psi_n\,ds, \tag{6b}$$

where σ and s denote the solution domain and its outer boundary respectively.

The solution for Stokes flow is obtained by finding the stationary value of equation (6a) or (6b). Taking the variation of (6a) with respect to ω and (6b) with respect to Ψ and equating to the corresponding variations of (5) yields

$$\iint \delta\omega[\nabla^2\Psi + \omega]\,d\sigma = \iint [-(\Psi_x\,\delta\omega_x + \Psi_y\,\delta\omega_y) + \omega\,\delta\omega]\,d\sigma + \int \delta\omega\Psi_n\,ds, \tag{7a}$$

$$\iint \delta\Psi[\nabla^2\omega]\,d\sigma = \iint -[\omega_x\,\delta\Psi_x + \omega_y\,\delta\Psi_y]\,d\sigma + \int \delta\Psi\omega_n ds. \tag{7b}$$

The variations $\delta\Psi$ and $\delta\omega$ are arbitrary except that

$$\delta\Psi = 0, \quad \text{when } \Psi \text{ is specified;}$$
$$\delta\omega = 0, \quad \text{when } \omega \text{ is specified.}$$

At solid wall boundaries Ψ is specified; thus equation (7b) becomes trivial since $\delta\Psi = 0$, and is replaced by the Dirichlet condition $\Psi = \bar{\Psi}(s)$.

The second boundary condition ($\Psi_n = \bar{\Psi}_n(s)$) is satisfied naturally by the contour integral of equation (7a). Note that since $\bar{\Psi}_n(s)$ is usually equal to zero, satisfying the no-slip condition becomes

trivial. Note that, although it is not necessary for stability to reverse the classical boundary conditions between Ψ and ω, this reversal makes the boundary condition very simple and contrasts with the method of Dhatt *et al.*[2] in which an approximate explicit representation for Ψ_n is needed, which could become cumbersome for complex geometries.

Weighted residual method for viscous flows with convection

Guidelines for the weighted residual formulation for the non-linear problem now become apparent. The weighted residual equations are

$$\iint W_1[\nabla^2\omega - Re(\Psi_y\omega_x - \Psi_x\omega_y)]\,d\sigma = 0, \tag{8a}$$

$$\iint W_2[\omega + \nabla^2\Psi]\,d\sigma = 0, \tag{8b}$$

where W_1 and W_2 are weight functions. At solid wall boundaries equation (8a) must be dropped; thus W_1 must be zero at these boundaries, whereas there are no restrictions on W_2. Equation (8a) is then replaced by the condition $\Psi = \bar{\Psi}(s)$. Application of Green's theorem to equations (8) yields

$$\iint [W_{1x}\omega_x + W_{1y}\omega_y + W_1 Re(\Psi_y\omega_x - \Psi_x\omega_y)]\,d\sigma = \int_{C_3} W_1\omega_n\,ds = 0, \tag{9a}$$

$$\iint [W_2\omega - W_{2x}\Psi_x - W_{2y}\Psi_y]\,d\sigma = \int_{C_1+C_3} W_2\Psi_n\,ds. \tag{9b}$$

Using the Newton–Raphson method, the linearized equations for the changes in the variables $\Delta\Psi$ and $\Delta\omega$ are

$$\iint \{W_{1x}(\Delta\omega)_x + W_{1y}(\Delta\omega_y) + W_1 Re[\Psi_y(\Delta\omega)_x + \omega_x(\Delta\Psi)_y - \Psi_x(\Delta\omega)_y - \omega_y(\Delta\Psi)_x]\}\,d\sigma = R_1, \tag{10a}$$

$$\iint \{W_2\Delta\omega - W_{2x}(\Delta\Psi)_x - W_{2y}(\Delta\Psi)_y\}\,d\sigma = -\int_{C_1+C_3} \Psi_n\,ds + R_2, \tag{10b}$$

where R is the residual. Equations (10a) and (10b) are solved with the unknowns Ψ and ω approximated as

$$\Psi = \sum_i N_i^{\Psi}\Psi_i, \quad \text{thus } \Delta\Psi = \sum_i N_i^{\Psi}\Delta\Psi_i, \tag{11a}$$

$$\omega = \sum_i N_i^{\omega}\omega_i, \quad \text{thus } \Delta\omega = \sum_i N_i^{\omega}\Delta\omega_i, \tag{11b}$$

where N^{Ψ} and N^{ω} are finite element shape functions and i is the number of degrees of freedom of the particular variable.

Equations (10) are first solved for creeping flow ($Re = 0$) with high Re solutions obtained by incrementing the value of Re and using the solution at a lower value as the starting point. A relaxed convergence criterion is used at intermediate values of Re.

Several elements (Figure 2) were tried. They were:

1. 8-node element with 16 degrees of freedom ($8\Psi, 8\omega$).

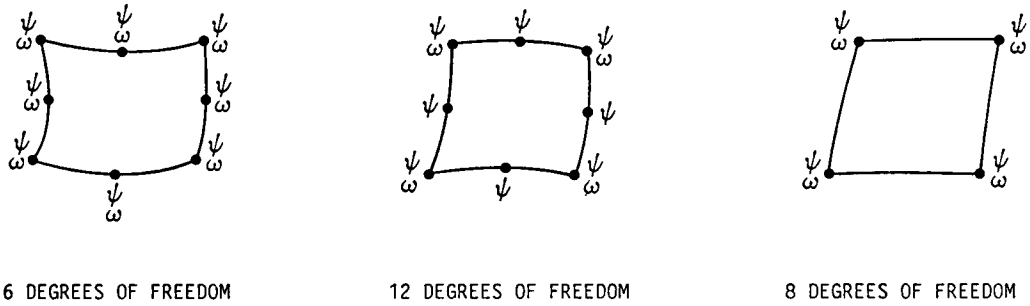

Figure 2. Elements used

2. 8-node element with 12 degrees of freedom $(8\Psi, 4\omega)$
3. 4-node element with 8 degrees of freedom $(4\Psi, 4\omega)$.

With the first element, all shape functions and weight functions were quadratic; with the third element all shape functions and weight functions were linear; with the second element the shape function N^{ω} was linear whereas N^{Ψ} was quadratic, and two options were considered for the weight functions: W_1 quadratic and W_2 linear, or W_1 linear and W_2 quadratic.

The pressure equation

The components of the momentum equation written in terms of pressure are

$$p_x = -[(u^2)_x + (uv)_y - (1/Re)(\nabla^2 u)] \equiv f, \tag{12a}$$

$$p_y = -[(v^2)_y + (uv)_x - (1/Re)(\nabla^2 v)] \equiv g. \tag{12b}$$

By taking the divergence of these equations, the following equation for pressure results:

$$\nabla^2 p = f_x + g_y. \tag{13}$$

This equation has, in the literature, been reduced to

$$\nabla^2 p = 2(\Psi_{xy}\Psi_{yy} - \Psi_{xy}^2). \tag{14}$$

Various methods[4,5] have been used to solve for the pressure from either of these two equations. However, in the present work, we adopt a method,[3] that leads to simple natural boundary conditions, demonstrating the advantages of a finite element formulation.

The weighted residual integral for equation (13) is

$$\int\int W\{p_{xx} - f_x + p_{yy} - g_y\}\,\mathrm{d}x\mathrm{d}y = 0 \tag{15}$$

Integrating the complete equation by parts yields

$$\int\int \{W_x(p_x - f) + W_y(p_y - g)\}\,\mathrm{d}\sigma = \int W(p_x - f)\,\mathrm{d}y + \int W(p_y - g)\,\mathrm{d}x. \tag{16}$$

Note that the contour integrals just contain the momentum equations and thus vanish as a natural boundary condition in the finite element formulation. The pressure level is determined by setting the pressure equal to zero at one point on the inlet. Equation (16) is solved using standard techniques once the stream function is known.

RESULTS AND DISCUSSION

Choice of element

Tests were done initially to determine which elements and corresponding weight functions worked best. The test case was the rapidly diffusing duct shown in Figure 1. At all but extremely low *Re* the flow would separate in such a duct.

Unless otherwise noted, *Re* is based on the duct height and average velocity at the inlet.

Figure 3 shows the convergence histories of two types of elements at *Re* ranging from 0 to 100. The elements were the 16 degree of freedom (DOF) element and the 12 degree of freedom element with quadratic W_2 (Ψ equation) and linear W_1 (ω equation). The 12 DOF elements with linear W_2 and quadratic W_1 never converged. The 8 DOF element was not considered until later in the study. The results indicate that the convergence properties of the 16 DOF element deteriorate rapidly as the Reynolds number increases, almost going unstable at $Re = 100$. On the other hand, the 12 DOF element converges rapidly at all Reynolds numbers. For both cases an under-relaxation factor of 0·6 was found to yield the best convergence.

Based on these initial tests, formulations using the 16 DOF element and the 12 DOF element with quadratic W_1 and linear W_2 were abandoned.

Later in the study tests were performed with 8 DOF elements and these were found to take the exact same number of iterations as the 12 DOF elements for tests on the same grid. The results were, however, less accurate and the savings in computer time were not great; thus all results presented henceforth are with the 12 DOF element.

It should be noted that Dhatt *et al.*[2] also used the same 12 DOF element. No mention was made of any other elements tried. It is believed that this choice of element made possible the high *Re* solutions presented in that reference.

Flow in a driven cavity

Driven cavity flow is a classical problem studied by many researchers to determine the effectiveness of Navier–Stokes solvers. This problem features a square domain where the lid is moving and all other sides are stationary.

Figure 4 shows equivorticity and streamline plots for $Re = 400$. Figure 5 shows centre-line velocities and includes the results of a number of other researchers as surveyed by Olson.[6]

The results of the current study agree well with previous work.

High Reynolds number separated flow

The performance of the method at high *Re* was considered next. The geometry and grid used are shown in Figure 6; the flow at the inlet was fully developed. The flow will separate in the trough along the hub but will otherwise remain attached. Converged solutions were obtained for Reynolds numbers up to 100,000, although at such a Reynolds number the laminar solution has little physical significance.

Plots of streamlines in the separated zone for $Re = 10{,}000$ are shown in Figure 7. The results look qualitatively correct, but even at this Reynolds number the flow would be turbulent.

Inviscid limit

The method was tested at $Re = \infty$ to demonstrate that there are no Reynolds number

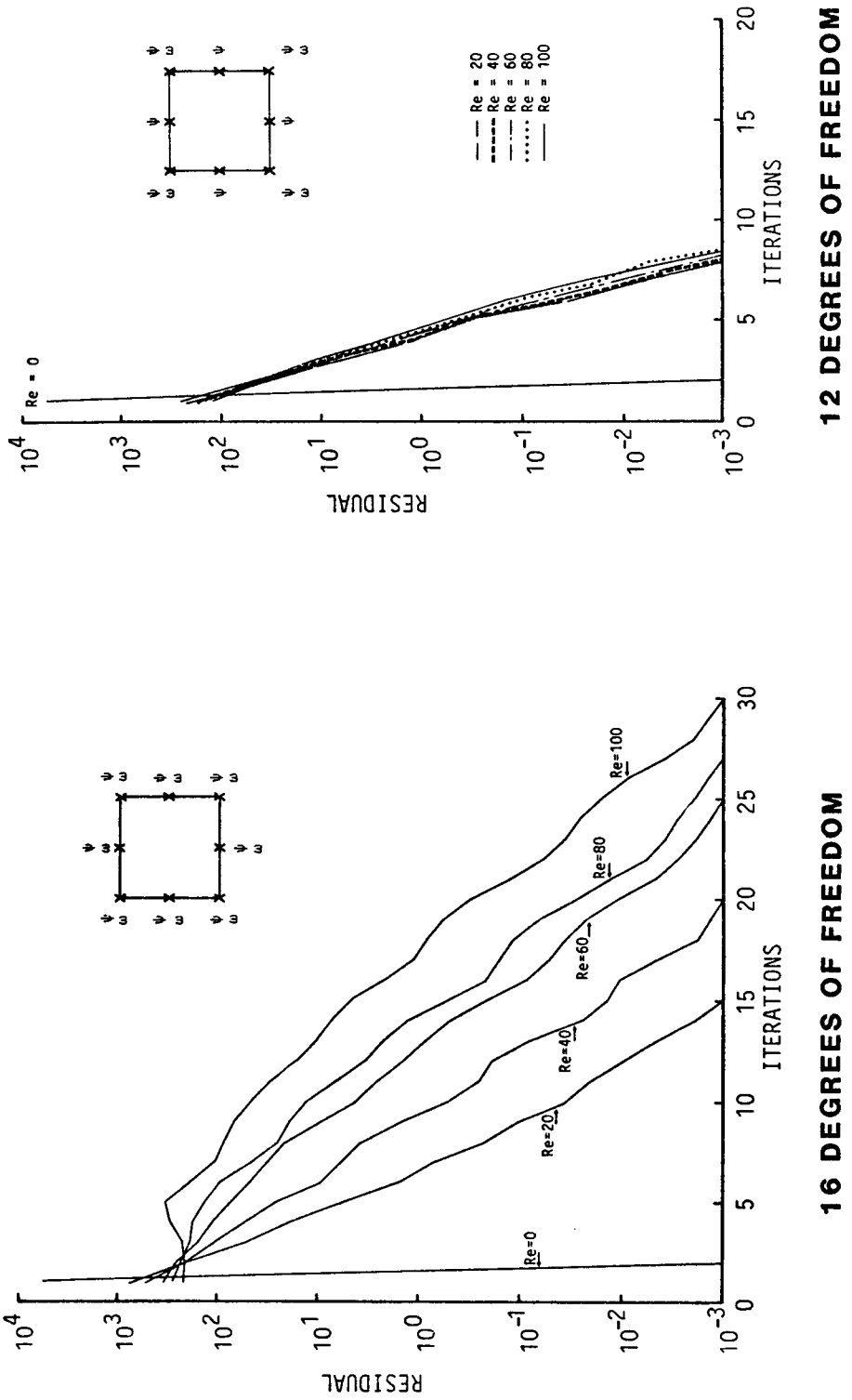

Figure 3. Convergence histories for the 16 DOF and 12 DOF elements

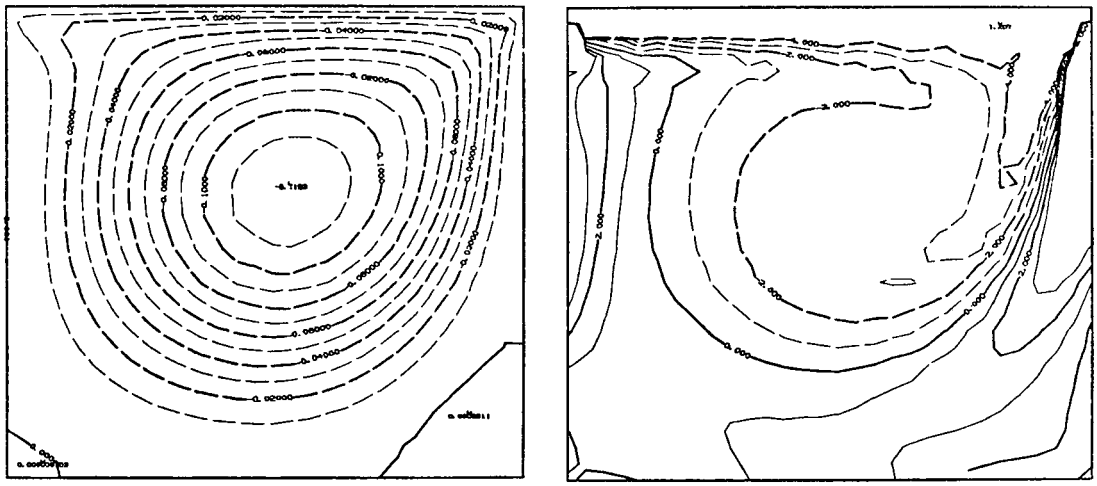

Figure 4. Streamlines and equivorticity lines for driven cavity, $Re = 400$

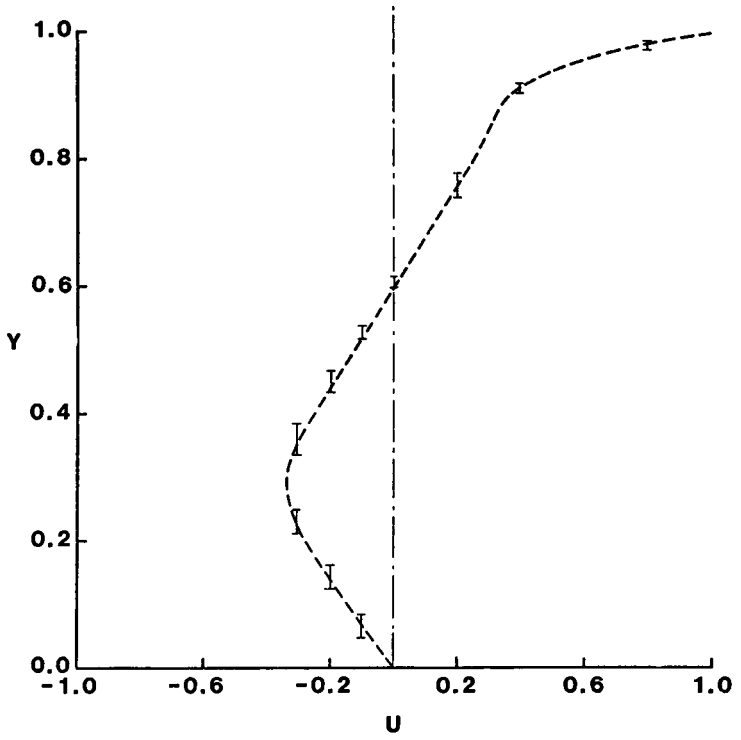

Figure 5. Centre-line velocities for driven cavity, $Re = 400$.
I Range of solutions from Olson[6] excluding high and low curves

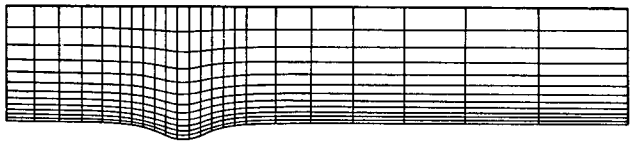

Figure 6. Geometry and grid for high *Re* test

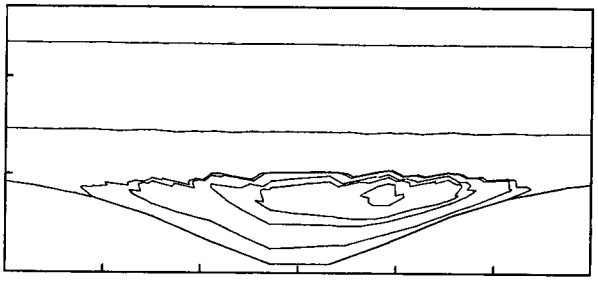

Figure 7. Streamlines in trough, $Re = 10{,}000$

Figure 8. Geometry and grid for inviscid test case

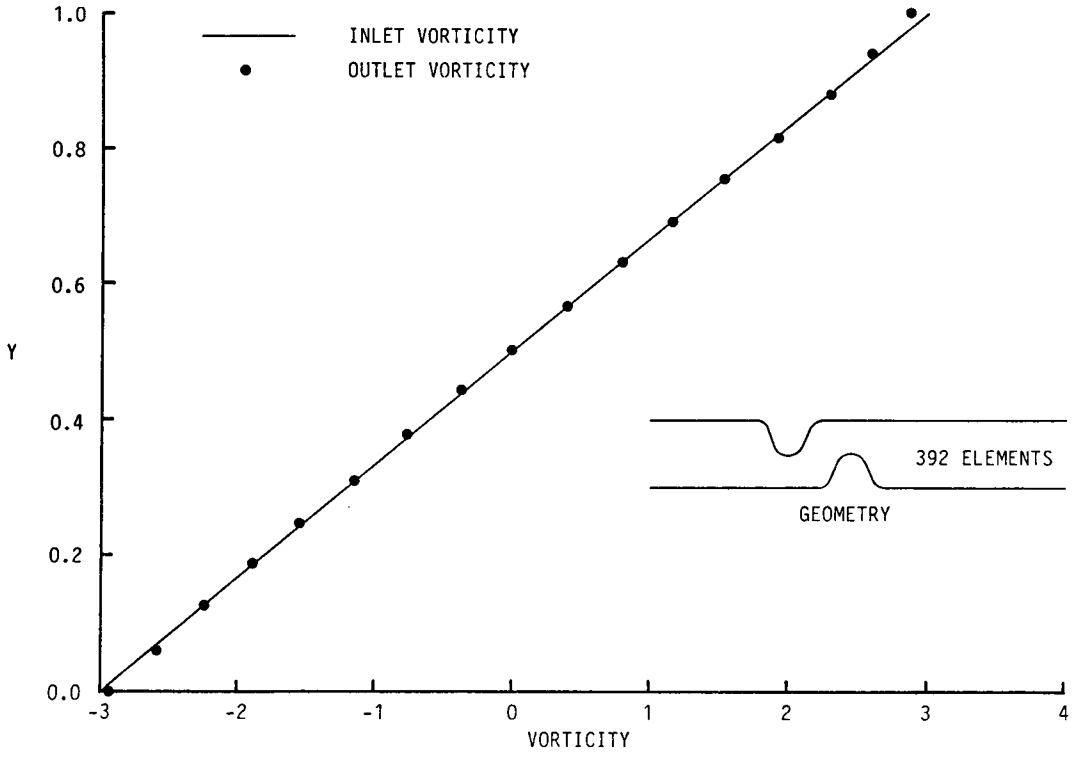

Figure 9. Inlet and outlet vorticity profiles for inviscid test case

restrictions on the algorithm and also to show that false diffusion is not inherent in the algorithm. The test geometry was the strongly curved and constricted duct shown in Figure 8. This geometry forces the flow to make several sharp turns and to accelerate and decelerate rapidly in succession. The inlet had a linear vorticity profile. With no false diffusion the profile at the exit of the duct should be identical to that at the inlet. Note that as mentioned in the finite element formulation section it is not necessary to reverse the imposition of the boundary conditions between Ψ and ω. For the inviscid case therefore, in order to drop the no-slip condition, we impose the no-penetration condition directly on Ψ. Figure 9 compares inlet and exit vorticity profiles. As can be seen the profiles are virtually identical.

Pressure solutions

Eight-node, isoparametric elements were used for this problem. Note that the right-hand side of (12) contains second derivatives of velocity, so three derivatives of stream function are required. Fortunately this term is divided by *Re* so for most problems of interest it is small. As a test case, fully developed flow through a duct was considered. The test was performed at low $Re(150)$ to investigate if the coarse representation of the second derivatives of velocity would create a problem. Theoretical[7] and computed pressure coefficients, along the duct are presented in Figure 10. The agreement is quite good.

Effect of grids

The accuracy of the solutions obtained was, of course, dependent on the grid used. It was found that for very coarse grids the algorithm could diverge. As the grid was refined, converged solutions could be obtained, but sometimes these would be oscillatory, especially at high *Re*, in flows with large streamwise gradients. Further refinements would remove these oscillations. These observations are similar to those noted in Reference 8.

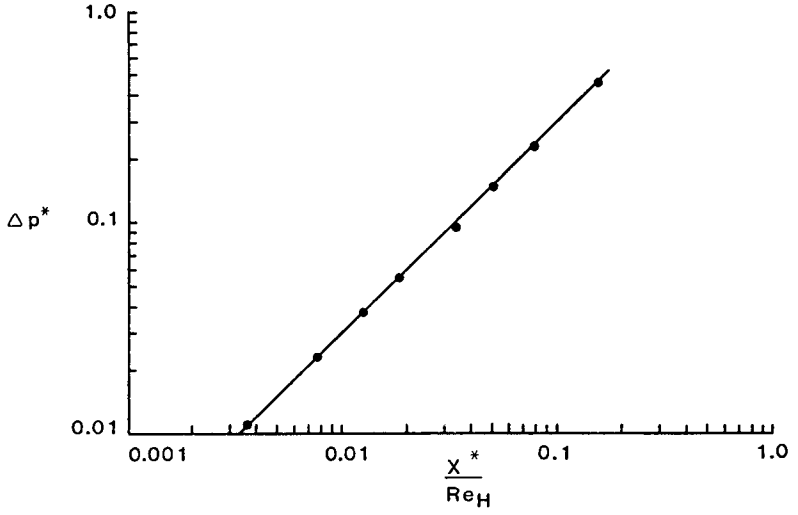

Figure 10. Theoretical and computed pressure coefficients. Theoretical: $\Delta p^* = 3x^*/Re_H$; $p^* = p/\rho\ U^2 avg$, $x^* = x/H$, H = (duct height)/2. ● this study

CONCLUDING REMARKS

The use of wall vorticity formulae for stream function/vorticity formulations of the Navier–Stokes equation is not necessary, as an analysis of Stokes flow shows that the no-slip boundary condition is satisfied naturally by the stream function equation, and the no-penetration condition replaces the vorticity transport equation, obviating the need for the traditional calculations of wall vorticity. This formulation gives accurate results at all Reynolds numbers provided certain elements are used. Specifically, linear interpolation for ω is required, and either linear or quadratic interpolation for Ψ can be used.

A novel pressure field calculation method was applied and it has been shown to be particularly suited to finite element formulations.

REFERENCES

1. A. Campion-Renson and M. J. Crochet, 'On the stream function vorticity finite element solutions of Navier–Stokes equations', *Int. j. numer. methods eng.*, **12**, 1809–1818 (1978).
2. G. Dhatt, B. K. Fomo and C. A. Bourque, "A ψ–ω finite element formulation for the Navier–Stokes equations', *Int. j. numer. methods eng.*, **17**, 199–212 (1981).
3. M. M. Hafez, W. G. Habashi and P. L. Kotiuga, 'Conservative calculations of non-isentropic potential flows', *AIAA Paper 84-1182*, AIAA/SAE/ASME, 20th Joint Propulsion Conference, Cincinnati, June 1984.
4. P. J. Roache, *Computational Fluid Dynamics*, Hermosa Publishers, Alburquerque, N.M., 1976.
5. S. Tuann and M. D. Olson, 'A transient finite element solution method for the Navier–Stokes equations', *Computers and Fluids*, **6**, 131–152 (1978).
6. M. D. Olson, 'Comparison problem no. 1, recirculating flow in a square cavity', *Report No. 22*, Structures Research Series, University of British Columbia, Vancouver, B.C., 1979.
7. T. Cebeci and P. Bradshaw, *Momentum Transfer in Boundary Layers*, McGraw-Hill, 1977.
8. P. M. Gresho and R. E. Lee, 'Don't suppress the wiggles—they're telling you something', *Computers and Fluids*, **9**, 233–253 (1981).